LETTERS

Adaptive coding of visual information in neural populations

Diego A. Gutnisky[1] & Valentin Dragoi[1]

Our perception of the environment relies on the capacity of neural networks to adapt rapidly to changes in incoming stimuli[1–4]. It is increasingly being realized that the neural code is adaptive[5], that is, sensory neurons change their responses and selectivity in a dynamic manner to match the changes in input stimuli[1,2,5]. Understanding how rapid exposure, or adaptation, to a stimulus of fixed structure changes information processing by cortical networks is essential for understanding the relationship between sensory coding and behaviour[5–8]. Physiological investigations of adaptation have contributed greatly to our understanding of how individual sensory neurons change their responses to influence stimulus coding[2,9–12], yet whether and how adaptation affects information coding in neural populations is unknown. Here we examine how brief adaptation (on the timescale of visual fixation)[2,9,10] influences the structure of interneuronal correlations and the accuracy of population coding in the macaque (*Macaca mulatta*) primary visual cortex (V1). We find that brief adaptation to a stimulus of fixed structure reorganizes the distribution of correlations across the entire network by selectively reducing their mean and variability. The post-adaptation changes in neuronal correlations are associated with specific, stimulus-dependent changes in the efficiency of the population code, and are consistent with changes in perceptual performance after adaptation[2,13,14]. Our results have implications beyond the predictions of current theories of sensory coding, suggesting that brief adaptation improves the accuracy of population coding to optimize neuronal performance during natural viewing.

Understanding how adaptation influences population coding requires an understanding of how adaptation changes the structure of interneuronal correlations across the network. Indeed, during the past decade, it has become increasingly understood that the trial-by-trial variability in neuronal responses, or 'noise', is not independent, but that it exhibits correlations[15,16]. This implies that the accuracy of the population code must depend on the distribution of noise correlations across the network[17–19]. Theoretically, it has been proposed that adaptation would reduce neuronal correlations, and hence redundancy[20,21], to improve stimulus coding[1]. In reality, exactly how the structure of correlations across a population of neurons is affected by adaptation, and how it influences the efficiency of coding, is unknown.

We address this issue in the context of the macaque primary visual cortex (V1), in which adaptation has been shown previously to induce changes in the response magnitude and selectivity of individual neurons[2,5,9–11]. We focus on a particular, rapid form of adaptation that is believed to occur spontaneously during visual fixation when cortical cells are exposed to redundant information for hundreds of milliseconds[2,9]. Our hypothesis is that rapid adaptation changes the structure of noise correlations in V1 and increases the amount of information in a population code in a way that is consistent with perceptual performance.

Responses to dynamic test stimuli in area V1 of a fixating monkey were recorded before and after brief (400-ms) adaptation to a sine-wave grating of fixed orientation (Fig. 1a). We used a movie sequence as the test stimulus (see Methods), in which each frame was a sine-wave grating of pseudorandom orientation flashed at 60 Hz. The stimulus was fixed across trials and covered multiple neuronal receptive fields (Supplementary Fig. 1). We measured noise correlations (trial-to-trial covariation of spike counts of a cell pair) between pairs of nearby neurons ($n = 423$ pairs). We confirmed previous findings[16] that noise correlations are independent of stimulus orientation; only 5% of the pairs exhibited a significant relationship between the correlation coefficient and stimulus orientation (see Methods).

Figure 1b shows an example of a pair of cells preferring nearby orientations that exhibit a strong reduction in correlations after adaptation (the pre-adaptation condition is labelled 'control'). Across the population, we found an overall post-adaptation decrease in the absolute correlation coefficients that was significant both for positive (mean reduction 22%, $P < 10^{-8}$, Wilcoxon signed rank test) and for negative (mean reduction 74%, $P < 10^{-5}$) coefficients (Fig. 1c; the post-adaptation reduction in correlations is significant in each monkey, Supplementary Fig. 2). This reduction in correlation strength is also found in cells that exhibit positive correlations before adaptation and negative correlations after adaptation (mean reduction 73%, $P < 10^{-6}$) and negative correlations before adaptation and positive correlations after adaptation (mean reduction 42%, $P < 0.005$). Overall, correlation coefficients decayed exponentially with the difference ($\Delta\theta$) in the cells' preferred orientation[22]; Supplementary Fig. 3a shows that adaptation reduces the peak and slope of the exponential decay of correlation coefficients. We further examined whether the decrease in correlations after adaptation could be due to the small (5.8%), but significant ($P < 10^{-6}$), reduction in mean firing rates (Supplementary Fig. 1). However, we found no relationship between the mean changes in firing rates after adaptation and the changes in correlation coefficients[23] (Fig. 1d, $P > 0.3$, Pearson correlation).

Because adaptation is an orientation-specific phenomenon[2,3,10,11], we reasoned that the degree of decorrelation would depend on the relationship between the adapting stimulus and the preferred orientation of the cells in a pair. We therefore selected the cell pairs that preferred nearby orientations ($\Delta\theta < 30^\circ$), and compared the mean correlation coefficients before and after adaptation to stimuli of different orientation; we defined $\Delta\phi$ as the minimum difference between the adapting stimulus and the preferred orientation of each cell in a pair (Fig. 1e; see Methods and Supplementary Fig. 4). There is a strong reduction in correlations (Fig. 1f) for adapting stimuli near ($\Delta\phi \leq 30^\circ$, 31%, $P < 0.005$; Wilcoxon rank sum test) and far ($\Delta\phi > 60^\circ$), 43%, $P < 0.0005$) relative to the orientation of the cell pair, but intermediate adaptation ($30^\circ < \Delta\phi \leq 60^\circ$) was ineffective at reducing correlations (19%; $P > 0.1$).

[1]Department of Neurobiology and Anatomy, University of Texas-Houston Medical School, Houston, Texas 77030, USA.

These results indicate that brief adaptation reduces the strength of correlations in an orientation-asymmetric manner. We quantified the orientation dependency of this decorrelation by estimating the probability density function (pdf) of correlations, before and after adaptation, as a function of $\Delta\theta$ and $\Delta\phi$ using the kernel density estimation technique (see Supplementary Information). Contrary to the common belief that adaptation would only influence the responses of cells of similar preferred orientation (but consistent with Fig. 1f), we found a non-monotonic decorrelation profile (Fig. 2a)—that is, cells of similar ($\Delta\theta < 30^\circ$) and largely dissimilar ($\Delta\theta > 60^\circ$) orientation preference exhibit significant decorrelation, whereas cells with $\Delta\theta$ between 30° and 60° show only a weak decrease in correlations, both for near and far adaptation. This is shown in Fig. 2b, in which an adaptation decorrelation index is used to represent the magnitude of post-adaptation changes in absolute correlations; Supplementary Fig. 5 demonstrates the temporal stability of the decorrelation.

The changes in correlation structure after adaptation are described not only by changes in mean correlation coefficients but also by changes in the variability of correlations. Although it has been theoretically suggested that a small variability of correlations could increase coding efficiency[24], exactly how the variability of correlations influences population coding is unknown. Figure 3 shows that adaptation reduces not only the strength but also the variability of correlations (see also Supplementary Fig. 3b), both for near and for far adaptation. We explored this issue by estimating the pdf of correlations for pairs of cells with $\Delta\theta$ between 0° and 30° (small $\Delta\theta$), between 30° and 60° (intermediate $\Delta\theta$), and between 60° and 90° (large $\Delta\theta$). Figure 3d–f illustrates representative examples in which the adapting stimulus is near the preferred orientation of at least one of the cells in the pair ($\Delta\phi \leq 30^\circ$) or far from both cells ($\Delta\phi > 30^\circ$). For small $\Delta\theta$ (Fig. 3d), the post-adaptation pdf is sharper and shifted to the left relative to the pdf before adaptation. That is, there is both a significant decorrelation ($P < 0.0001$) and a reduction in correlation variability after adaptation. For intermediate $\Delta\theta$ (Fig. 3e), only far adaptation ($\Delta\phi > 30^\circ$) induces a significant decorrelation ($P < 0.001$). Contrary to expectation, for large $\Delta\theta$ (Fig. 3f), the adaptation-induced reduction in the mean and variability of correlations is even larger than that observed in cells preferring nearby orientations.

Together, these results raise the issue of whether the changes in the strength and variability of noise correlations after adaptation would affect the efficiency of the population code. We therefore computed network efficiency by estimating the Fisher information as the upper limit with which any decoding mechanism can extract information about stimulus orientation[17,18]. Consistent with the fact that second-order statistics are able to capture most of the variability of the population response[25], we assumed that the joint neuronal responses to stimulus orientation can be described by a multivariate gaussian defined by the mean firing rate and covariance matrix[17,18]. Fisher information was computed by assuming, first, that adaptation changes only the mean correlations, and second, both the mean

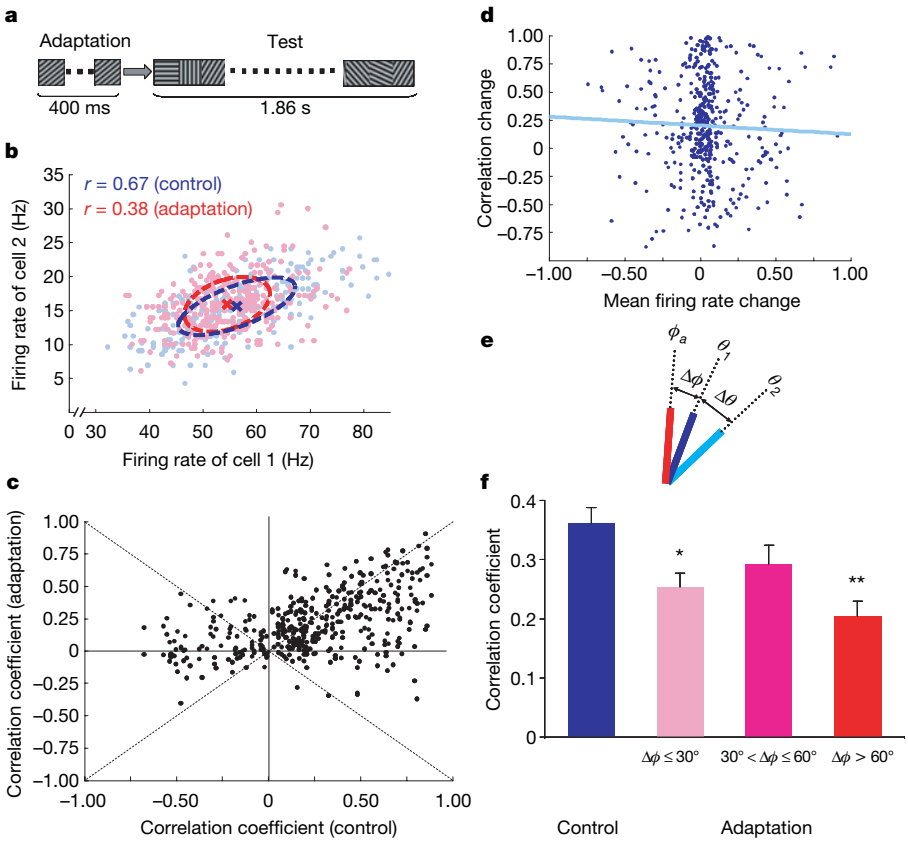

Figure 1 | Adaptation-induced response decorrelation in V1. **a**, Schematic representation of the stimulus sequence: an adapting stimulus of fixed orientation was presented for 400 ms and was followed by a 60-Hz test stimulus of random orientation presented for 1.86 s. **b**, Scatter plot showing the trial-by-trial responses of two cells recorded simultaneously. Each dot represents the firing rates of both cells in a given trial. The dotted ellipses represent the two-dimensional gaussian fits of the firing rate distributions during control and adaptation (crosses represent the means). '*r*' represents the correlation coefficient. **c**, Correlation coefficients for the population of cell pairs. Each dot represents the correlation coefficient for a pair of cells during control and adaptation (irrespective of the difference in preferred orientation). **d**, The post-adaptation changes in correlations cannot be attributed to the changes in the geometric mean firing rates of the cells in a pair ($P > 0.3$). The light blue line represents the linear regression fit. **e**, Schematic representing the preferred orientations of the cells in a pair (θ_1 and θ_2) and the adapting orientation (ϕ_a). $\Delta\theta$ and $\Delta\phi$ are defined in the text. **f**, The reduction in the mean correlation coefficients after adaptation depends on the adapting orientation (for pairs for which $\Delta\phi < 30^\circ$). All panels are based on the correlation analysis of $n = 423$ cell pairs ($\Delta\theta < 30^\circ$, 223 pairs; $\Delta\theta > 30^\circ$, 200 pairs). Error bars represent s.e.m. (*$P < 0.005$; **$P < 0.0005$).

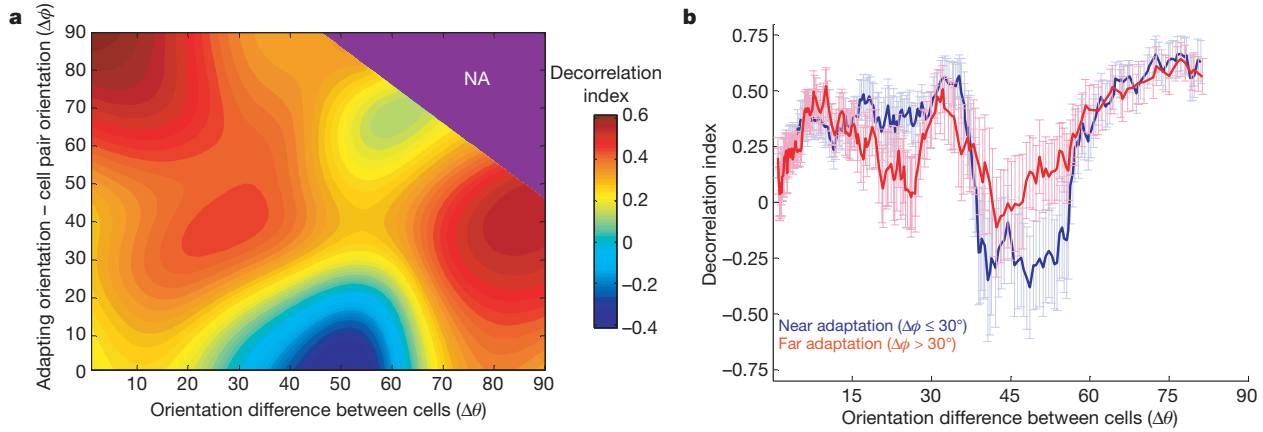

Figure 2 | Rapid adaptation changes the structure of interneuronal correlations. **a**, Decorrelation index as a function of the difference between the preferred orientations of the cells in a pair ($\Delta\theta$) and the minimum difference between the adapting orientation and that of each cell ($\Delta\phi$). The region of possible ($\Delta\theta$, $\Delta\phi$) pairs is described by $\Delta\phi + \Delta\theta \leq 135^\circ$ (although $\Delta\phi$ varies between 0° and 90°, $\Delta\theta$ is not completely independent of $\Delta\phi$). **b**, Adaptation decorrelates V1 responses in an orientation-asymmetric manner. Pairs were grouped depending on whether $\Delta\phi$ is smaller (near adaptation) or greater (far adaptation) than 30°; this ensures that the number of pairs in each category is approximately the same (46% of pairs had $\Delta\phi < 30^\circ$ and 54% of pairs had $\Delta\phi > 30^\circ$). The decorrelation index was calculated using the experimentally measured pairwise correlations in a sliding window of 20 points on the *x*-axis. Error bars represent s.e.m.

and variability of correlations (using the pdfs in Fig. 3a–c). Figure 4a shows that whereas the post-adaptation reduction in mean correlations caused a 25% improvement in the network orientation discriminability threshold, if both the changes in the mean and variability of correlations are taken into account the post-adaptation discrimination threshold is improved by 40%. Interestingly, for small populations, the post-adaptation network performance is slightly better than that of uncorrelated (independent) neurons, possibly due to a reduction in correlation variability[24].

The fact that adaptation changes interneuronal correlations in an orientation-asymmetric manner (Fig. 2) could cause the network efficiency to depend on the relationship between the adapting and test orientations. Indeed, we found that test stimuli similar or largely dissimilar with respect to the adapting orientation cause the largest improvement in coding efficiency. As shown in Fig. 4b, brief adaptation caused an almost fourfold increase in Fisher information when the network discriminated stimuli of similar and largely dissimilar orientation relative to the adapting stimulus, and a threefold increase

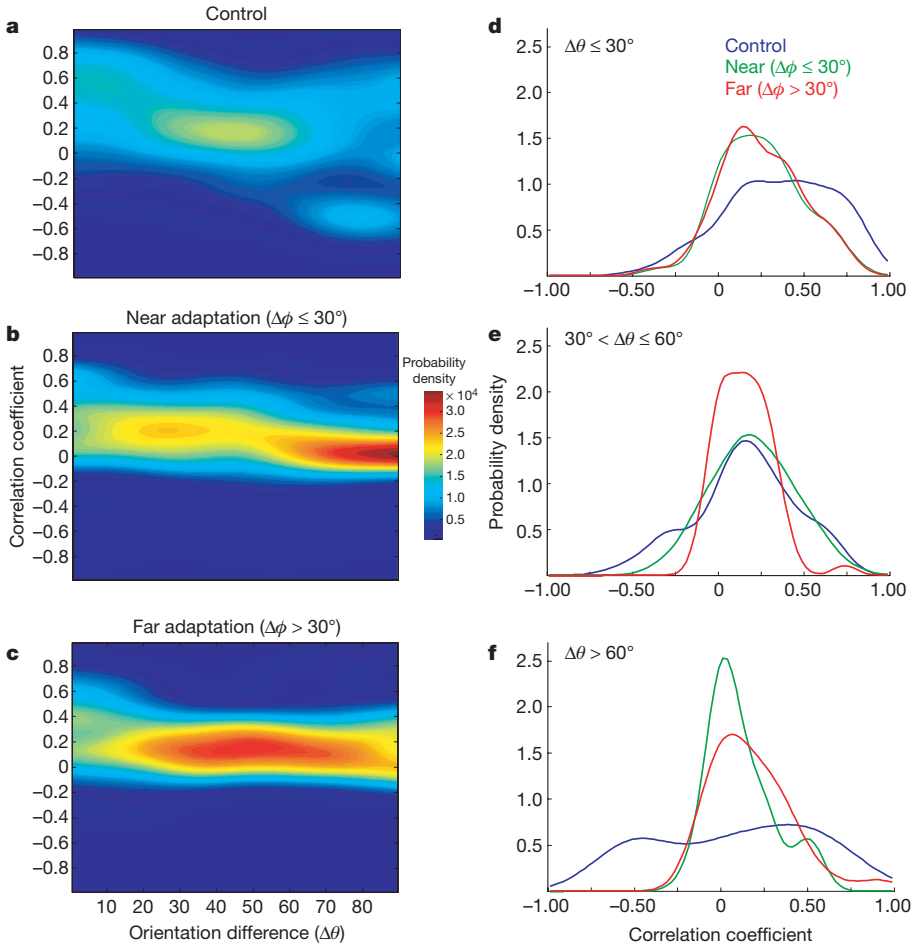

Figure 3 | Rapid adaptation changes the mean and variability of correlations. **a–c**, Probability density functions of correlations in control and adaptation (near, $\Delta\phi \leq 30^\circ$; far, $\Delta\phi > 30^\circ$) as a function of $\Delta\theta$. Both near and far adaptation reduces the variability of correlations. **d–f**, Probability density functions of correlation coefficients in control and adaptation in different $\Delta\theta$ bins ($<30^\circ$, 30°–60°, and $>60^\circ$). Adaptation decreases the mean and variability of correlations for small and large $\Delta\theta$ values.

in Fisher information for the discrimination of intermediate orientations. This is consistent with the larger reduction in the mean and variability of correlations for small and large $\Delta\theta$ ($<30^\circ$ and $>60^\circ$) relative to intermediate orientations ($\Delta\theta$ between 30° and 60°; Fig. 3d–f). Although these results may seem surprising, they are in agreement with human psychophysical data reporting that brief adaptation improves orientation discrimination near and far from the adapting orientation[2,13]. Importantly, we also found that the increase in population coding efficiency through decorrelation would be equivalent to an overall post-adaptation increase in firing rates of approximately 55%.

In addition to noise correlations, the population code is also characterized by signal correlations[26]—correlations in the neurons' average responses to a stimulus set. Rapid adaptation causes repulsive shifts in the neurons' orientation tuning curves and changes in firing rates[2,11] (Supplementary Fig. 6) to influence signal correlations. By examining the affect of the adaptation-induced changes in noise and signal correlations on coding efficiency (Fig. 4b), we found that, in agreement with psychophysical studies[2,13,14], the enhancement in network performance after adaptation is orientation-specific. Although these results have been obtained by computing correlations throughout the stimulus presentation, they also hold when noise correlations are measured on the timescale of visual fixation, during the first 400 ms of stimulus presentation (Supplementary Fig. 7). Thus, the post-adaptation improvement in network performance may influence sensory coding during natural viewing.

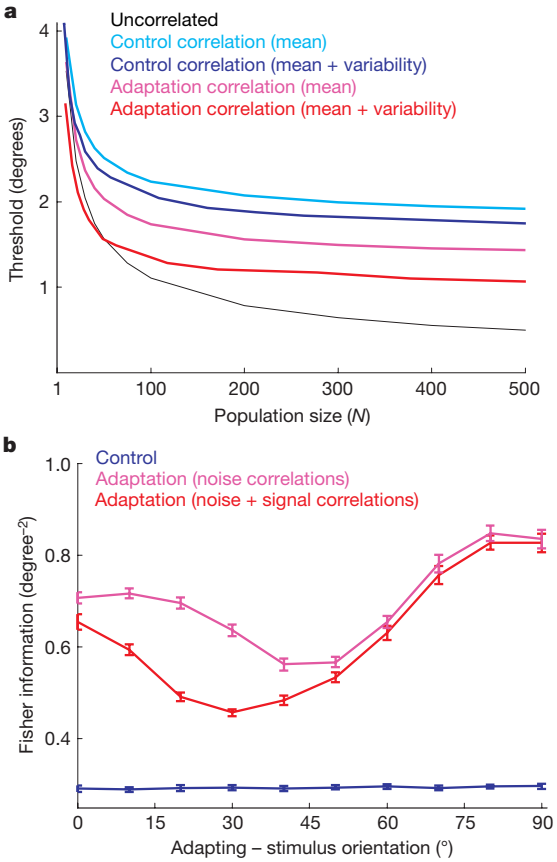

Figure 4 | Rapid adaptation enhances the efficiency of population coding. **a**, Adaptation increases the orientation discrimination performance of a neural population of variable size. Light blue and light red curves, adaptation changes only the mean correlation coefficients; dark blue and dark red curves, adaptation changes both the mean and variability of correlations. **b**, The efficiency of population coding (Fisher information) depends on $\Delta\theta$ and the adapting orientation (fixed at 0°; abscissa represents the test orientation). In control trials, Fisher information is independent of the test orientation. Post-adaptation changes in noise correlations cause the largest improvement in network performance when test stimuli are similar or largely dissimilar with respect to the adapting orientation. Combining the effects of noise and signal correlations yields a more pronounced U-shape profile of Fisher information. The error bars represent s.e.m.

We have demonstrated the functional significance of rapid adaptation by V1 networks for the coding of image features. Theoretically, adaptation has been proposed to reduce redundancy in sensory neurons, possibly by decorrelating responses, to improve coding efficiency[1,4]. However, in addition to the lack of experimental support, theories proposing the decorrelation hypothesis were unable to predict the changes in correlations across the entire network engaged in sensory computations. We provide empirical evidence that adaptation causes both a selective reduction in the strength and variability of correlations and an improvement in the efficiency of population coding. These results are consistent with the 'efficient coding hypothesis'[1,4]—that is, sensory neurons are adapted to the statistical properties of the stimuli that they are exposed to (Supplementary Fig. 8a, b)—and with psychophysical changes in human discrimination performance after adaptation (Supplementary Fig. 8c). We further propose that adaptation takes advantage of the rapid sequence of fixations during natural viewing to optimize image-discrimination performance in real time[2,27].

Our results argue that the visual system uses a metabolically inexpensive solution (selective decorrelation) to adapt neural responses to the statistics of the input stimuli and to improve coding efficiency. This raises the issue of whether decorrelation is an advantageous coding strategy in the visual cortex. Whereas selective decorrelation improves sensory discriminations by increasing network efficiency and possibly the organization of cell ensembles (Supplementary Fig. 9), it could be detrimental for other types of information processing. For instance, theoretical studies have suggested that temporally decorrelated inputs are transmitted less efficiently than correlated inputs[28]. Indeed, it is well known that in addition to sensory discriminations, the visual system is often required to perform other complex computations, such as contour grouping[29] or figure-ground segregation[30], which may require strong correlations between neurons. Hence, the fact that we did not observe a complete, homogeneous, decorrelation of responses in V1 could constitute a trade-off between distinct optimization goals during sensory processing[6].

METHODS SUMMARY

All experiments were performed in accordance with protocols approved by NIH. Multiple single-unit recordings were performed from V1 of two fixating monkeys (*Macaca mulatta*). Stimuli were presented so that they covered the centre of the neurons' receptive fields. In control trials, movie strips[2] were presented for ~1.86 s (16 orientations × 7 repeats at 60 Hz; random spatial phase). In adaptation trials, movies were preceded by a 400-ms grating of fixed orientation. The Pearson correlation coefficient of spike counts, R_{sc}, of two cells is defined as:

$$R_{sc} = \frac{\sum_{i=1}^{N} (r_1^i - \bar{r}_1)\cdot(r_2^i - \bar{r}_2)}{\sigma_1 \cdot \sigma_2}$$

where N is the number of trials, r_j^i is the firing rate of cell 'j' in trial 'i' averaged over the entire stimulus sequence, and σ is standard deviation of the responses. Correlation coefficients after adaptation depend on three variables: the adapting orientation, ϕ_a, and the preferred orientation of the cells in a pair, θ_1 and θ_2. To ensure that the parameter space is adequately sampled, the distance between the adapting orientation and the preferred orientation of one of the cells was held constant while varying the relative difference between the two cells' preferred orientations ($\Delta\theta$). We defined $\Delta\phi$ as the minimum difference between the adapting stimulus and the preferred orientation of each cell in a pair, that is, $\Delta\phi = \min(|\phi_a - \theta_1|, |\phi_a - \theta_2|)$. We define an adapting stimulus 'near' to a cell pair when the adapting orientation is $<30^\circ$ relative to at least one of the cells in the pair. Similarly, a 'far' adapting stimulus is oriented at least 30° away from both cells.

We calculated a decorrelation index as the percentage change in absolute correlation coefficient:

$$DI = \frac{|R_{control}| - |R_{adaptation}|}{|R_{control}|}$$

where R_i represents the correlation coefficients measured in condition 'i'. The

Monte Carlo simulations, kernel density estimation and Fisher information calculations are explained in the Methods and Supplementary Information.

Full Methods and any associated references are available in the online version of the paper at www.nature.com/nature.

Received 7 May 2007; accepted 9 January 2008.

1. Barlow, H. B. in *Sensory Communication* (ed. Rosenblith, W. A.) 217–234 (MIT, Cambridge, Massachusetts, 1961).
2. Dragoi, V., Sharma, J., Miller, E. K. & Sur, M. Dynamics of neuronal sensitivity in visual cortex and local feature discrimination. *Nature Neurosci.* **5,** 883–891 (2002).
3. Dragoi, V., Turcu, C. M. & Sur, M. Stability of cortical responses and the statistics of natural scenes. *Neuron* **32,** 1181–1192 (2001).
4. Simoncelli, E. P. Vision and the statistics of the visual environment. *Curr. Opin. Neurobiol.* **13,** 144–149 (2003).
5. Sharpee, T. O. *et al.* Adaptive filtering enhances information transmission in visual cortex. *Nature* **439,** 936–942 (2006).
6. Schwabe, L. & Obermayer, K. Rapid adaptation and efficient coding. *Biosystems* **67,** 239–244 (2002).
7. Wainwright, M. J. Visual adaptation as optimal information transmission. *Vision Res.* **39,** 3960–3974 (1999).
8. Vinje, W. E. & Gallant, J. L. Sparse coding and decorrelation in primary visual cortex during natural vision. *Science* **287,** 1273–1276 (2000).
9. Muller, J. R., Metha, A. B., Krauskopf, J. & Lennie, P. Rapid adaptation in visual cortex to the structure of images. *Science* **285,** 1405–1408 (1999).
10. Felsen, G. *et al.* Dynamic modification of cortical orientation tuning mediated by recurrent connections. *Neuron* **36,** 945–954 (2002).
11. Dragoi, V., Sharma, J. & Sur, M. Adaptation-induced plasticity of orientation tuning in adult visual cortex. *Neuron* **28,** 287–298 (2000).
12. Kohn, A. & Movshon, J. A. Neuronal adaptation to visual motion in area MT of the macaque. *Neuron* **39,** 681–691 (2003).
13. Clifford, C. W., Wyatt, A. M., Arnold, D. H., Smith, S. T. & Wenderoth, P. Orthogonal adaptation improves orientation discrimination. *Vision Res.* **41,** 151–159 (2001).
14. Regan, D. & Beverley, K. I. Postadaptation orientation discrimination. *J. Opt. Soc. Am.* **2,** 147–155 (1985).
15. Zohary, E., Shadlen, M. N. & Newsome, W. T. Correlated neuronal discharge rate and its implications for psychophysical performance. *Nature* **370,** 140–143 (1994).
16. Kohn, A. & Smith, M. A. Stimulus dependence of neuronal correlation in primary visual cortex of the macaque. *J. Neurosci.* **25,** 3661–3673 (2005).
17. Abbott, L. F. & Dayan, P. The effect of correlated variability on the accuracy of a population code. *Neural Comput.* **11,** 91–101 (1999).
18. Sompolinsky, H., Yoon, H., Kang, K. J. & Shamir, M. Population coding in neuronal systems with correlated noise. *Phys. Rev. E* **64,** 051904 (2001).
19. Pouget, A., Dayan, P. & Zemel, R. Information processing with population codes. *Nature Rev. Neurosci.* **1,** 125–132 (2000).
20. Reich, D. S., Mechler, F. & Victor, J. D. Independent and redundant information in nearby cortical neurons. *Science* **294,** 2566–2568 (2001).
21. Schneidman, E., Bialek, W. & Berry, M. J. II. Synergy, redundancy, and independence in population codes. *J. Neurosci.* **23,** 11539–11553 (2003).
22. Ts'o, D. Y., Gilbert, C. D. & Wiesel, T. N. Relationships between horizontal interactions and functional architecture in cat striate cortex as revealed by cross-correlation analysis. *J. Neurosci.* **6,** 1160–1170 (1986).
23. de la Rocha, J., Doiron, B., Shea-Brown, E., Josić, K. & Reyes, A. Correlation between neural spike trains increases with firing rate *Nature* **448,** 802 (2007).
24. Wilke, S. D. & Eurich, C. W. On the functional role of noise correlations in the nervous system. *Neurocomputing* **44–46,** 1023–1028 (2002).
25. Schneidman, E., Berry, M. J. II, Segev, R. & Bialek, W. Weak pairwise correlations imply strongly correlated network states in a neural population. *Nature* **440,** 1007–1012 (2006).
26. Averbeck, B. B. & Lee, D. Coding and transmission of information by neural ensembles. *Trends Neurosci.* **27,** 225–230 (2004).
27. Dragoi, V. & Sur, M. Image structure at the center of gaze during free viewing. *J. Cogn. Neurosci.* **18,** 737–748 (2006).
28. Salinas, E. & Sejnowski, T. J. Impact of correlated synaptic input on output firing rate and variability in simple neuronal models. *J. Neurosci.* **20,** 6193–6209 (2000).
29. Roelfsema, P. R., Lamme, V. A. & Spekreijse, H. Synchrony and covariation of firing rates in the primary visual cortex during contour grouping. *Nature Neurosci.* **7,** 982–991 (2004).
30. van der Togt, C., Kalitzin, S., Spekreijse, H., Lamme, V. A. & Super, H. Synchrony dynamics in monkey V1 predict success in visual detection. *Cereb. Cortex* **16,** 136–148 (2006).

Supplementary Information is linked to the online version of the paper at www.nature.com/nature.

Acknowledgements We thank K. Josić for comments on the manuscript. This work was supported by the Pew Scholars Program, the James S. McDonnell Foundation and the National Eye Institute (V.D.).

Author Information Reprints and permissions information is available at www.nature.com/reprints. Correspondence and requests for materials should be addressed to V.D. (v.dragoi@uth.tmc.edu).

METHODS

Electrophysiological recordings. We used standard methods for single-unit extracellular recording as described previously[2]. Microelectrodes (tungsten/glass, 1–2 MΩ at 1 kHz, FHC Inc.) were advanced transdurally through stainless steel guide tubes into V1. We recorded up to 8 units simultaneously in each session at depths between 200 μm and 400 μm. Recording sites were located between 1 mm and 2 mm of each other; most of the neurons (>80%) were recorded on different electrodes. More than 80% of cells were complex cells. Single-unit isolation was assessed offline using waveform clustering based on parameters such as spike amplitude, timing, width, valley and peak. When a unit was isolated, its receptive field was mapped using an automatic procedure while the animal maintained fixation. Receptive field eccentricities ranged between 2° and 6° from the centre of gaze (receptive field positions were reconfirmed at the end of the experiments).

Monkeys were trained to fixate on a small spot (0.1°) presented on a video monitor placed 57 cm in front of the monkey. Once the animal achieved stable fixation for 100 ms, the visual stimulus was presented. Monkeys were required to hold fixation throughout stimulus presentation to earn a juice reward; the trial was automatically aborted if fixation instability exceeded 0.25° at any time during stimulus presentation. Eye position was continuously monitored using an infrared eye tracking system operating at 250 Hz (Iscan). The stimulus presentation, behavioural trials, and eye position control and recording were done with the Cortex software package (NIH). Stimuli were movie strips in which each frame consisted of a $5 \times 5°$ sine-wave grating of 2 cycles per degree spatial frequency and 75% contrast presented binocularly. In control trials, movies were presented for ~1.86 s (16 orientations × 7 repeats at 60 Hz; random spatial phase for each orientation); in adaptation trials, movies were preceded by a 400-ms grating of fixed orientation (we used between 250 and 300 control and adaptation trials). To increase the effectiveness of adaptation, we used drifting sine-wave gratings (temporal frequency of 3 Hz; similar spatial characteristics to the movie gratings) as adapting stimuli. (In pilot experiments, we found that drifting gratings typically evoked stronger adaptation than flashed stimuli.) Control and adaptation trials were grouped in blocks of trials; adaptation trials were followed by 'recovery' trials that were identical to the control trials. For our population of cell pairs, the control and recovery correlation coefficients were indistinguishable ($P > 0.1$, Wilcoxon signed rank test). Our choice of oriented stimuli (as opposed to natural images) is motivated by the fact that Fisher information and the efficiency of population coding can only be assessed by using parametric stimuli. To examine whether our results were affected by differences in the quality of fixation between control and adaptation conditions, we calculated the deviation of eye position and velocity along the vertical and horizontal axes during the movie sequence presentation. The average standard deviation of these measures was not statistically different in the control and adaptation conditions, $P > 0.1$, Student's *t*-test.

The cells' preferred orientation and orientation selectivity index (OSI) were computed every 8 ms using the reverse correlation method[2] (the mean OSI across the population was 0.29 and was similar to that reported in previous V1 studies[2,3,11]). The distribution of preferred orientations for the cells in our population and the range of adapting orientations ensured a uniform sampling of the orientation space (Supplementary Fig. 4).

Noise correlations. We presented the same movie stimulus (that is, the same pseudo-random orientation sequence, or 'frozen noise') in each control and adaptation trial. We measured the correlation coefficient for each of the 16 orientations at a given time lag (varied every 8 ms) and the geometric mean firing rate of the cell pair. We found that only 5% of pairs exhibited a significant relationship between the correlation coefficient (converted to *Z*-score through the Fisher transformation) and the evoked firing rate of the cell pair. Our stimulus allowed us to calculate noise correlations by pooling the neuronal responses to all the orientations present in the stimulus[16] (see Supplementary Information). Our choice of complex stimuli instead of simple oriented gratings is justified by our focus on rapid adaptation. Computing correlations by measuring neuronal responses using briefly flashed test stimuli of fixed orientation (lasting hundreds of milliseconds) would be inappropriate because these stimuli would significantly reduce firing rates (the neurons would adapt to the stimulus itself) to contaminate the noise correlation coefficients. Extracting only the (unadapted) spikes generated during the first 100 ms of stimulus presentation would not solve this problem because cells with low firing rates (<20 Hz) will fire, at most, two spikes to cause an unreliable estimation of the correlation coefficients. In contrast, our movie stimulus has the advantage that cells are continuously stimulated with a broad range of orientations, thus preventing the neurons to reduce their firing rates substantially during stimulus presentation.

Except for Fig. 1f, we binned our data into two groups: near ($\Delta\phi \leq 30°$) and far ($\Delta\phi > 30°$) adaptation. This is justified by the definition of $\Delta\phi$, which implies that not all ($\Delta\theta$, $\Delta\phi$) pairs are possible. For instance, for $\Delta\theta = 90°$, the maximum $\Delta\phi$ is 45°. We explored other alternative measures for $\Delta\phi$—for example, the sum of the differences between the adapting stimulus and the preferred orientations of each cell in a pair, or the distance between the adapting orientation and the mean orientation of the two cells in a pair—but did not find a significant difference from the results reported here (data not shown).

Monte Carlo simulations. We generated populations of cells with idealized gaussian tuning curves (baseline 5 Hz, peak 30 Hz, standard deviation 25°) uniformly spanning preferred orientations between 0° and 180°; we assumed a response variability of 15 Hz^2 that was independent of orientation. These parameters are consistent with the average tuning curve parameters of our population of V1 cells. In the first set of Monte Carlo simulations, we used only the mean correlation profile for both control and adaptation conditions. We assumed that the mean correlations depend only on the difference in the preferred orientation of the cells in a pair. We computed Fisher information for 500 populations of different size (between 10 and 500 neurons). In the second set of Monte Carlo simulations, we used the distribution probability of correlations (mean and variance) instead of the mean correlations. For each $\Delta\theta$, we estimated the correlation density function $p(R_{SC}|\Delta\theta)$ in the control case. In the adaptation condition, correlations depend on the difference between the adapting stimulus and the preferred orientation of the cells in a pair. We were therefore able to estimate the post-adaptation correlation density function $p(R_{SC}|\Delta\theta, \Delta\phi)$, and then sampled these distributions to obtain a set of covariance matrices for which we computed Fisher information.

Fisher information. The inverse of the Fisher information represents the lower limit of the variance of an unbiased estimator of stimulus orientation θ (the Cramer-Rao[31] bound). When the joint neural response is described by a multivariate gaussian (our assumption), Fisher information can be computed as[31,32]:

$$J(\theta) = f'(\theta)^T C^{-1}(\theta) f'(\theta) + \frac{1}{2} Tr\left[C'(\theta) C^{-1}(\theta) C'(\theta) C^{-1}(\theta)\right]$$

where $J(\theta)$ is the Fisher information, $f'(\theta)$ is the derivative of the tuning curve, $C(\theta)$ is the covariance matrix, *Tr* is the trace, and C' and f' are the first derivatives with respect to θ. The second term of the equation depends on the derivative of the covariance matrix $C'(\theta)$, and represents the information about the stimulus encoded in the variance of the neural responses. Because we found that the correlation matrix was independent of θ, and we assumed an additive gaussian noise model, the second term was ignored.

31. Kay, S. M. *Fundamentals of Statistical Signal Processing*. Prentice-Hall signal-processing series (PTR Prentice-Hall, Englewood Cliffs, 1993).
32. Dayan, P. & Abbott, L. F. *Theoretical Neuroscience: Computational and Mathematical Modeling of Neural Systems* 108–113 (Massachusetts Institute of Technology, Cambridge, Massachusetts, 2001).